



King Saud University
Arabian Journal of Chemistry

www.ksu.edu.sa
www.sciencedirect.com



ORIGINAL ARTICLE

Adsorption and corrosion inhibiting behavior of *Lannea coromandelica* leaf extract on mild steel corrosion

P. Muthukrishnan^a, B. Jeyaprabha^b, P. Prakash^{a,*}

^a Department of Chemistry, Thiagarajar College, Madurai 625009, India

^b Department of Civil Engineering, Fatima Michael College of Engineering & Technology, Madurai 625020, India

Received 28 January 2013; accepted 14 August 2013

KEYWORDS

Mild steel;
Lannea coromandelica;
SEM;
AFM;
Polarization;
Acid corrosion

Abstract *Lannea coromandelica* leaf extract (LCLE) as a corrosion inhibitor in 1 M H₂SO₄ was investigated by weight loss and electrochemical techniques. Inhibition efficiency of LCLE was found to increase with increasing concentration but decreased with increasing temperature. Polarization measurements revealed that the LCLE acted as a mixed type inhibitor. Nyquist plots showed that on increasing the LCLE concentration, the charge transfer resistance increased and the double layer capacitance decreased. The adsorption of LCLE on mild steel obeyed the Langmuir adsorption isotherm. FT-IR, XRD, SEM and AFM techniques confirmed the adsorption of LCLE on mild steel surface.

© 2013 Production and hosting by Elsevier B.V. on behalf of King Saud University.

1. Introduction

Acid solutions are widely used in industry for several processes such as acid pickling, industrial acid cleaning, acid descaling and oil well acidizing (Zhang and Hua, 2009). During the past decade, many techniques have been used to minimize the corrosion of iron due to attack by acids. One of the techniques for minimizing corrosion is the use of inhibitors (Ravi Chandran and Rajendran, 2005; Atul Kumar, 2008). Most of the corrosion inhibitors are organic compounds having hetero atoms

in their aromatic ring (N, S, O, P) or long chain carbon (Ebenso et al., 2008b; Eddy and Ebenso, 2008; Popova et al., 2004). Most of the synthetic chemicals are toxic to the environment. Due to the toxicity of some corrosion inhibitors, there has been increasing search for green corrosion inhibitors (Shahid, 2011). Most of the natural inhibitors are environmentally friendly, non-toxic, biodegradable, inexpensive and readily available in plenty (Lebrini et al., 2011; Okafor et al., 2008; El-Etre, 2007; Lecante et al., 2011; Satapathy et al., 2009). Corrosion inhibition of leaf extracts of *Occimum viridis*, *Telferia occidentalis*, *Azadirachta indica* and *Hibiscus sabdariffa* on mild steel in acidic solutions was investigated by Oguzie (2008). Other than the plant extracts, pure organic compounds extracted from natural products such as ascorbic acid (Goncalves and Mello, 2001), succinic acid (Amin et al., 2007), tryptamine (Moretti et al., 2004), caffeine (Fallavena et al., 2006), Pennyroyal oil (Bouyanzer et al., 2006), amino acids (Zhang et al., 2008) and caffeic acid (De Souza and Spinelli, 2009) have also been used for the inhibition of corrosion. An investigation has

* Corresponding author. Tel.: +91 9842993931; fax: +91 4522312375.

E-mail address: kmpprakash@gmail.com (P. Prakash).

Peer review under responsibility of King Saud University.



Production and hosting by Elsevier

been made in this present work on the corrosion of mild steel in 1 M H₂SO₄ using the extract of *Lannea coromandelica* as corrosion inhibitor by the weight loss method and the electrochemical method, FT-IR, XRD, SEM and AFM. Additionally, thermodynamic and kinetic parameters were calculated and discussed. *L. coromandelica* is an easily available plant in India. It belongs to the anacardiaceae family which is commonly known as the Indian Ash Tree. The extract of this plant contains numerous naturally environmental organic compounds. The genus of *L. coromandelica* is known to contain significant amounts of polyphenols including Flavonoids, Tannins, Terpinoids, Gums and polysaccharides (Avinash Kumar Reddy et al., 2011; Vadivel et al, 2012). The leaf of the plant is biodegradable and a renewable material. It has never been reported so far on the use of leaf extract of LC on the corrosion of mild steel in 1 M H₂SO₄.

2. Experimental

2.1. Preparation of the specimens

Composition of mild steel specimen was C: 0.13, Si: 0.18, P: 0.39, S: 0.04, Cu: 0.025 and balance Fe. The specimens were mechanically cut into sizes with 2.5 cm × 2.5 cm × 0.4 cm dimensions and abraded with different emery papers up to 4/0 grades. Each specimen was degreased by washing with acetone, dried at room temperature and preserved in a moisture-free desiccator. All chemicals and reagents were of analar grade. The concentration of test solution (1 M H₂SO₄) was prepared by using triple-distilled water and AR grade sulfuric acid.

2.2. Extraction of LCL extract

LC leaves were collected in and around Madurai, India. The leaves were dried, ground and soaked in bidistilled water for

24 h. After 24 h, the crude extracts were boiled, cooled and triple filtered. The amount of plant material extracted into solution was quantified by comparing the weight of dried residue with the initial weight of the dried plant material before extraction. From the respective stock solutions, inhibitor test solution was prepared in the concentration range from 50 to 250 mg/l.

2.3. Gravimetric experiments

Gravimetric experiment was conducted at different temperatures in the range 308–328 K for 12 h in 1 M H₂SO₄. The specimens were immersed in 100 ml of the respective inhibitor and test solutions in a thermostated bath. The specimens were weighed before and after immersion. The difference in weight was taken as the weight loss of mild steel. From the weight loss (ΔW), corrosion rate (λ) and the percentage of inhibition efficiency (IE%) were calculated using the following equation:

$$\lambda \text{ (mpy)} = 534 \times \Delta W / DAT \quad (1)$$

$$\text{IE\%} = (W_0 - W_1) / W_0 \times 100 \quad (2)$$

Here $\Delta W = (W_b - W_a)$, where W_b and W_a are the specimen weights before and after immersion in the tested solution, W_0 and W_1 are the weight loss of mild steel in the absence and presence of inhibitor respectively, D is the density of the iron (g/cm³), A is the area of the specimen in inch² and T is the period of immersion in hours.

2.4. Electrochemical measurements

Tafel polarization curves and Nyquist impedance curves were recorded using H and CH electrochemical workstation impedance Analyzer Model CHI 604D. A cell containing three compartments for electrode was used. The working polished mild steel electrode with exposed area of 0.5 cm² was immersed in

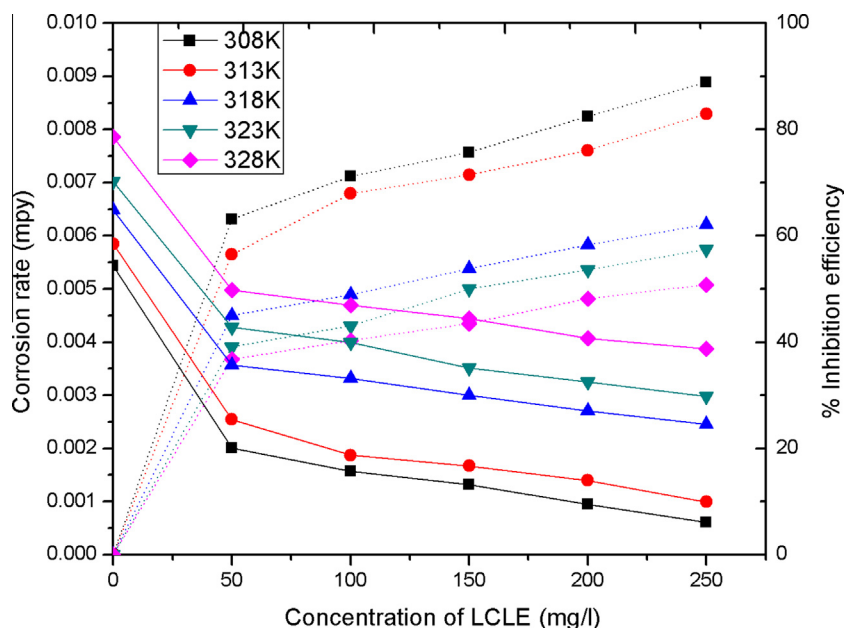


Figure 1 Corrosion rate and Inhibition efficiency of mild steel specimens immersed in 1 M H₂SO₄ with and without LCLE at 308, 313, 318, 323 and 328 K (-) corrosion rate (---) inhibition efficiency.

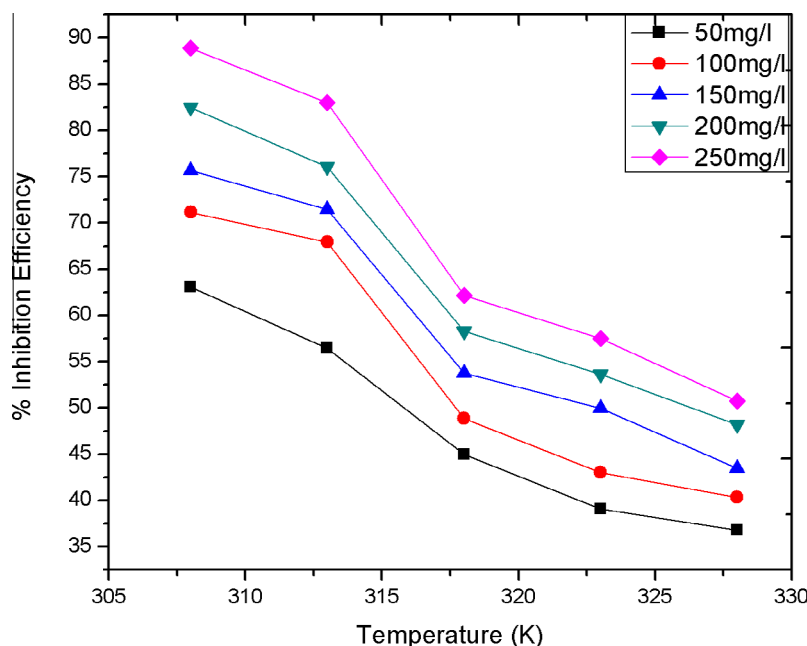


Figure 2 Inhibition efficiency versus temperature in the presence of different concentrations of LCLE.

a test solution. A platinum electrode and saturated calomel electrode were used as the counter and the reference electrode respectively. Before each potentiodynamic polarization (Tafel) and Electrochemical impedance spectroscopy (EIS) experiment, the electrode was allowed to corrode freely and its open-circuit potential was recorded. Potentiodynamic polarization curves were recorded from -200 to $+200$ mV_{SCE}, (versus OCP) with a scan rate of 1 mV s^{-1} . Electrochemical impedance spectroscopy measurements were performed in the frequency range of 0.1 Hz to 100 KHz . All electrochemical measurements were studied at 308 K using 100 ml of electro-

lyte ($1 \text{ M H}_2\text{SO}_4$) in stationary condition. Each experiment was repeated in triplicate to check the reproducibility of the data.

2.5. Surface analysis

2.5.1. Fourier Transform Infra-Red spectroscopy (FT-IR)

FT-IR spectra were recorded in SHIMADZU-FTIR-8400S spectrophotometer. One specimen for FT-IR characterization was the LCL extract. On the other hand, the mild steel specimens were immersed for 12 h in 100 ml of $1 \text{ M H}_2\text{SO}_4$ solution

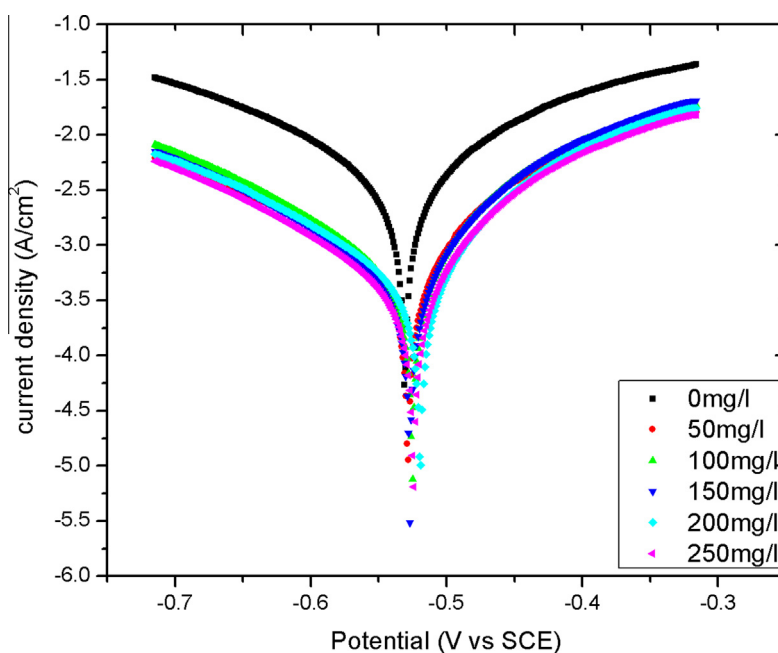
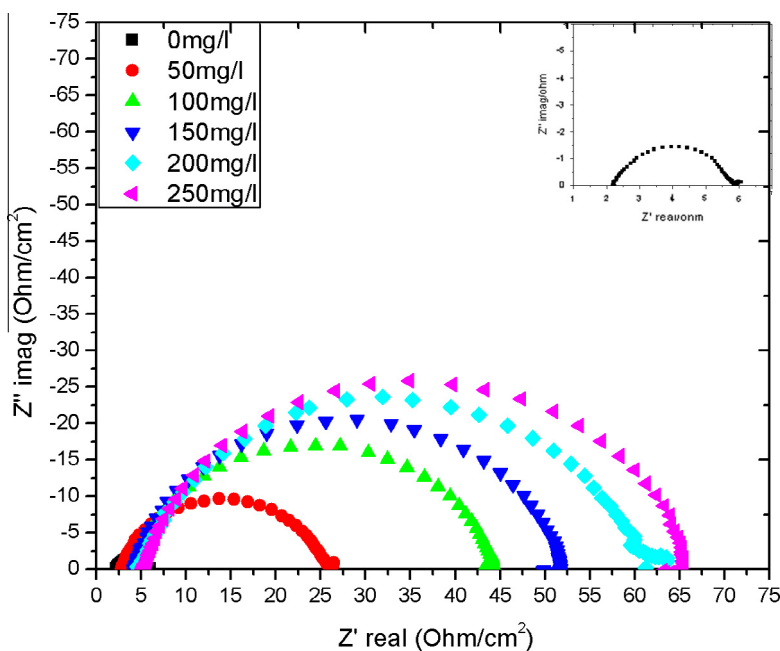


Figure 3 Tafel plots of mild steel immersed in $1 \text{ M H}_2\text{SO}_4$ with and without LCLE.

Table 1 Potentiodynamic polarization parameters for the corrosion of mild steel in 1 M H₂SO₄ containing different concentrations of LCLE.

C_{inh} (mg/l)	E_{corr} (mV)	i_{corr} ($\mu\text{A cm}^{-2}$)	b_c (mV/decade)	b_a (mV/decade)	R_p (Ωcm^2)	% IE
0	-531	4622.0	168.0	158.6	7.7	-
50	-504	880.4	161.0	143.8	37.5	81.0
100	-513	763.1	142.6	126.8	38.2	83.5
150	-512	645.7	140.1	119.4	43.4	86.0
200	-519	638.3	144.6	121.1	44.9	86.2
250	-506	531.8	142.1	122.0	53.7	88.5

**Figure 4** Nyquist plots for mild steel immersed in 1 M H₂SO₄ (■) (inset) and different concentrations of LCLE at 308 K.

containing 250 mg/l LCLE. After 12 h, the specimens were taken out and dried and then rubbed with a small amount of KBr powder and made into a disk.

2.5.2. X-ray diffraction studies

The nature of the protective film formed on the surface of the mild steel in acids in the presence of inhibitor for a period of 6 h was studied using XRD techniques. After 6 h, the specimens were taken out and dried. This film between metal/solution interfaces was analyzed by using X-ray diffractometer, Model (Phillips) X' pert.

Table 2 Electrochemical impedance parameters for mild steel in 1 M H₂SO₄ in the absence and presence of LCLE.

C_{inh} (mg/l)	R_s (Ωcm^2)	R_{ct} (Ωcm^2)	C_{dl} (F/cm ²)	% IE
0	2.2	3.7	2.9×10^{-2}	-
50	2.9	24.5	6.7×10^{-4}	84.9
100	4.3	38.1	2.4×10^{-4}	90.7
150	4.4	39.9	1.6×10^{-4}	92.2
200	4.8	47.3	1.1×10^{-4}	93.8
250	5.4	60.1	1.0×10^{-4}	93.8

2.5.3. SEM and AFM characterizations

The mild steel specimens were immersed in acid solutions in the absence and presence of optimum concentration of inhibitor for a period of 6 h. After 6 h, the specimens were taken out and dried. The nature of the surface film formed on the surface of the mild steel specimen was examined by using a JEOL (JSM 6390) Scanning Electron Microscope and Scanning probe microscope (Akilan Technology UK 5500 series).

2.6. Phytochemical studies

Phytochemical analysis of alkaloids, flavonoids, glucosides, carbohydrates, phenols, aminoacids, steroids, triterpenoids, saponins and tannins was carried out by using the methods of Brindha et al. (1977) and Harbone (1988).

3. Results and discussion

3.1. Effect of LCLE on corrosion rate of mild steel

The corrosion rate of mild steel in 1 M H₂SO₄ in the absence and presence of different concentrations of *L. coromandelica* leaf extracts was determined at 308–328 K. Fig. 1 shows the

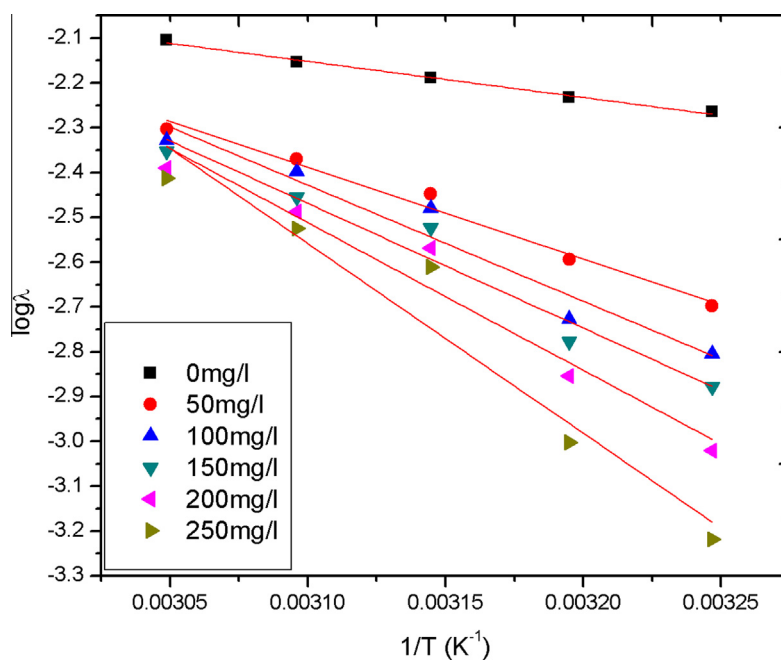


Figure 5 Arrhenius plot of $\log \lambda$ versus $1/T$ at different concentrations of LCLE.

effect of concentration of LCLE on the corrosion rate and inhibition efficiency of mild steel in 1 M H_2SO_4 with and without the LCL extract. From the graph, it is clear that the corrosion rate of mild steel decreased in the presence of LCLE when compared to the uninhibited acid solution. The corrosion rate also decreased with increasing concentration of the inhibitor. This indicated that the corrosion of mild steel was inhibited by extract of LCL in 1 M H_2SO_4 and that the extent of corrosion inhibition depended on the amount of the LCL present in H_2SO_4 . Maximum inhibition efficiency

was found to be 89% at 250 mg/l (308 K), which indicated that LCLE was a good inhibitor in 1 M H_2SO_4 . Fig. 2 shows the plot of inhibition efficiency against different temperatures with different concentrations of inhibitors. From the plots, it was very clear that the inhibitor efficiency decreased with increase of temperature which was due to the desorption of LCLE from the surface of mild steel (Sanja Martinez and Ivica Stern, 2002; Ebenso et al., 2008a, 2009; Bentiss et al., 2007; Oguzie et al., 2005; Ita and Offiong, 1999; Bouklah et al., 2006).

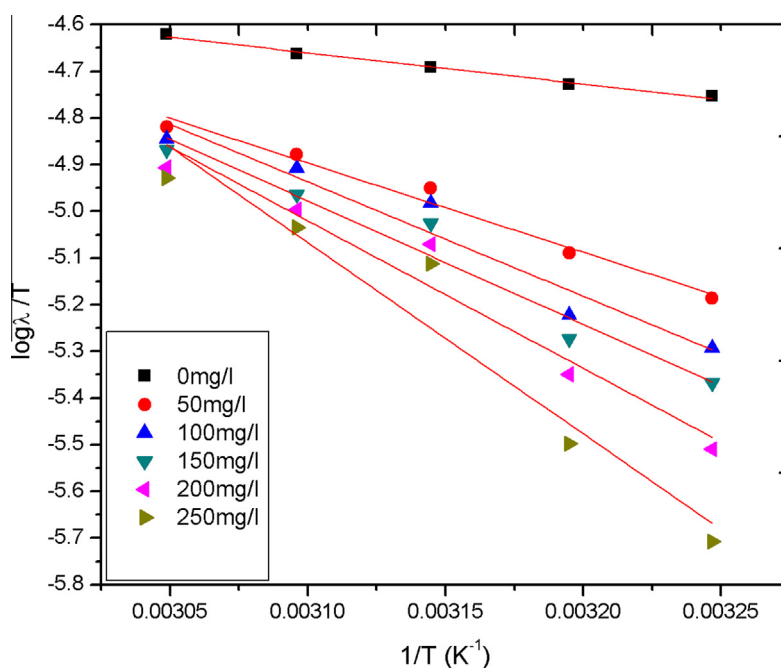


Figure 6 Transition state plots $\log \lambda/T$ versus $1/T$ at different concentrations of LCLE.

Table 3 Corrosion kinetic parameters for mild steel in 1 M H₂SO₄ in the absence and presence of different concentrations of LCLE.

C_{inh} (mg/l)	E_a (kJ/mol)	ΔH^* (kJ/mol)	$-\Delta S^*$ (J/mol/K)
0	15.4	12.8	148.0
50	39.3	36.6	177.7
100	49.6	47.0	146.4
150	53.3	50.7	135.7
200	63.2	60.5	106.0
250	81.2	78.5	51.2

3.2. Electrochemical measurements

The potentiodynamic polarization curves of mild steel immersed in the absence and presence of inhibitor are shown in Fig 3. The corrosion parameters namely corrosion potential (E_{corr}), corrosion current (I_{corr}), cathodic slope (b_c), anodic slope (b_a), Linear polarization resistance (LPR) and percentage of inhibition efficiency calculated from Tafel plots are given in Table 1. The inhibition efficiency is defined as

$$IE\% = (i_{corr}^0 - i_{corr}/i_{corr}^0) \times 100 \quad (3)$$

where i_{corr}^0 and i_{corr} are the corrosion current density values without and with inhibitor respectively. In the present study, the maximum shift E_{corr} values are in the range of 27 mV. From the values, it is confirmed that the LCLE acts as mixed type of inhibitor (Singh and Quraishi, 2010). Table 1 shows that the values of b_c were changed less than b_a values. This suggested that the anodic reaction was controlled predominantly than the cathodic one at all concentrations. Moreover in the presence of the inhibitor system, the corrosion current decreased from 4622 to 531.8 $\mu\text{A}/\text{cm}^2$ and LPR values increased from 7.7 to 53.7 ohm cm^2 . These observations confirmed that

Table 4 Langmuir adsorption parameters and free energy of adsorption of LCLE as inhibitor on the surface of mild steel.

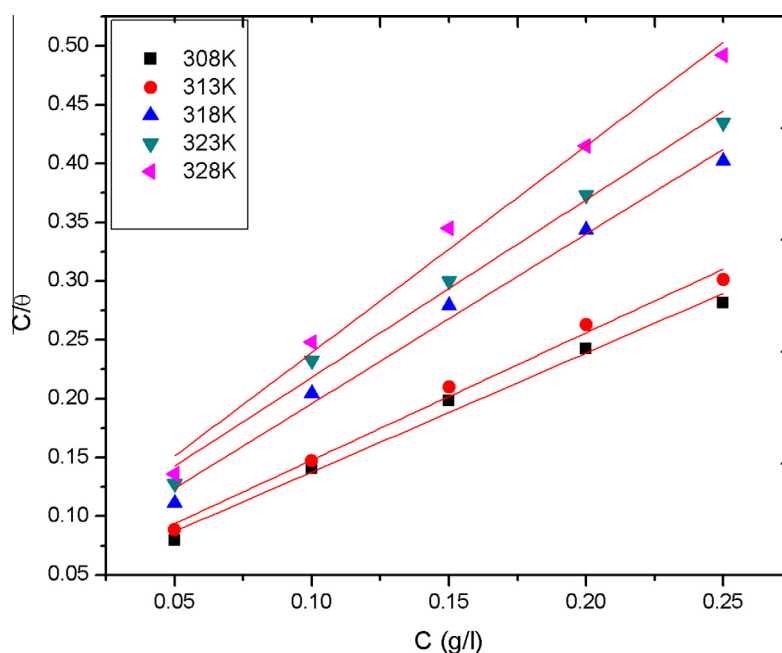
Temp (K)	$-\Delta G_{ads}^\circ$ (kJ/mol)	$-\Delta H_{ads}^\circ$ (kJ/mol)	$-\Delta S_{ads}^\circ$ (J/mol/K)	R^2
308	18.9		29.5	0.990
313	18.9	27.9	28.9	0.992
318	18.5		29.8	0.991
323	18.0		30.7	0.990
328	18.5		28.8	0.990

addition of LCLE to 1 M H₂SO₄ solution will reduce anodic dissolution of mild steel more than the cathodic hydrogen evolution reaction (Musa et al., 2012).

Impedance diagrams obtained for mild steel in 1 M H₂SO₄ in the presence and absence of the inhibitors are shown in Fig. 4. The impedance parameters such as R_s , R_{ct} , C_{dl} and f_{max} derived from Nyquist plots are given in Table 2. The charge transfer resistance increased with an increase in the concentration of inhibitor in acid solution. In the impedance studies, IE% was calculated as:

$$IE\% = (R_{ct(inh)} - R_{ct}/R_{ct(inh)}) \times 100 \quad (4)$$

where R_{ct} and $R_{ct(inh)}$ are uninhibited and inhibited charge transfer resistance respectively. The diameter of Nyquist plots increased on increasing the concentration of LCLE which indicated the strengthening of inhibitor film (Taleb and Mehad, 2011). As the concentration of inhibitor increased, charge transfer resistance enhanced and decreased the double layer capacitance values. This was due to the adsorption of LCLE on the metal surface leading to the formation of a protective layer on the electrode surface and decreased the extent of dissolution reaction (Vinod kumar et al., 2010; Sobhi et al., 2012). These results were in very good agreement with both weight

**Figure 7** Langmuir adsorption isotherm for mild steel in 1 M H₂SO₄ containing different concentrations of LCLE at 308–328 K.

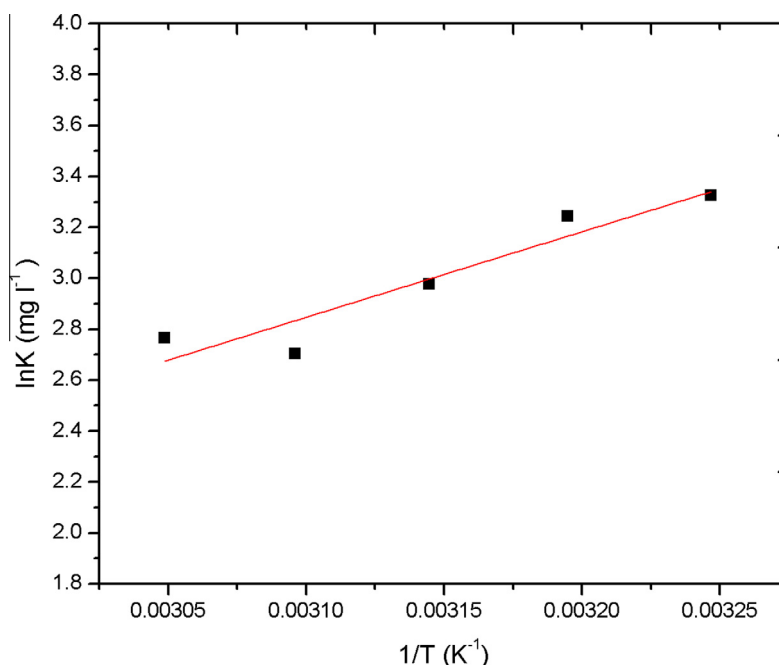


Figure 8 Plot of $\ln K$ vs $1/T$ for the adsorption of LCLE at mild steel/sulfuric acid interface.

loss and polarization data and could be attributed to decreased local dielectric constant and increased thickness of the electrical double layer (Ibrahim and Habbab, 2011).

3.3. Thermodynamic considerations

The thermodynamic parameters such as the apparent activation energy E_a , the enthalpy of activation ΔH^* and the entropy of activation ΔS^* for corrosion of mild steel in 1 M H_2SO_4 solutions in the absence and presence of LCLE at 308–328 K were calculated from the Arrhenius equation:

$$\lambda = A \exp(-E_a/RT) \quad (5)$$

Taking the logarithm of both sides of Eq. (5), Eq. (6) could be obtained

$$\log \lambda = \log A - E_a/2.303RT \quad (6)$$

The change of enthalpy $\{\Delta H^*\}$ and entropy $\{\Delta S^*\}$ for the formation of activated complex in the transition state was obtained from the transition state equation.

$$\log \lambda/T = \{(\log R/hN + (\Delta S^*/2.303R)) - \Delta H^*/2.303RT\} \quad (7)$$

where λ is the corrosion rate, A is the pre-exponential factor, h is the Planck's constant, N is the Avogadro's number, E_a is the apparent activation energy, R is the gas constant ($R = 8.314 \text{ Jmol}^{-1} \text{ K}^{-1}$) and T is the absolute temperature.

A plot of $\log \lambda$ vs $1/T$ gave a straight line with slope of the line $(-E_a/2.303R)$ and intercept $(\log A)$ as shown in Fig. 5. The values of E_a were determined in solutions containing extracts of LCLE and found to be higher than uninhibited solution. The increase in E_a in the presence of LCLE could be interpreted as physical adsorption (Obot et al., 2012). A plot of $\log \lambda/T$ vs $1/T$ (Fig. 6) gave a straight line with slope of the line $(-\Delta H^*/2.303R)$ and an intercept $(\log R/hN + (\Delta S^*/2.303R))$

from which the values of ΔH^* and ΔS^* were calculated and summarized in Table 3. From these data, it was found that the thermodynamic parameters, ΔH^* and ΔS^* of dissolution reaction of mild steel in 1 M H_2SO_4 in the presence of LCLE were higher than uninhibited solution. The positive signs of the enthalpies ΔH^* reflected the endothermic nature of the steel dissolution process (Guan et al., 2004). The values of ΔS^* in the absence and presence of the tested inhibitor were negative, which indicated that the activated complex in the rate determining step represented an association rather than dissociation step, meaning that a decrease in disordering takes place on going from reactants to the activated complex (Soltani et al., 2010; Gomma and Wahdan, 1995; Behpour et al., 2011).

3.4. Adsorption isotherm

In general the adsorption isotherm provides essential information on the adsorption of inhibitor on metal surface. The θ values of different concentrations of inhibitor were tested by fitting to various isotherms including Frumkin, Langmuir, Temkin, Freundlich, Bockris-Swinkles and Flory Huggins isotherms. In the present study, the results fitted best the Langmuir adsorption isotherm, which is given by

$$C/\theta = 1/K_{\text{ads}} + C \quad (8)$$

where K_{ads} is the equilibrium constant of the adsorption process, C is the concentration inhibitor and θ is the surface coverage. The best fitted straight line was obtained for the plot of C/θ vs C (g/l) with slope of almost unity (Fig. 7). This behavior indicated that the adsorption of LCLE on mild steel surface obeyed the Langmuir adsorption isotherm meaning that there was no interaction between the adsorbed species (Behpour et al., 2011).

The free energy values of adsorption (ΔG_{ads}) of LCLE on mild steel surface were calculated using Eq. (9).

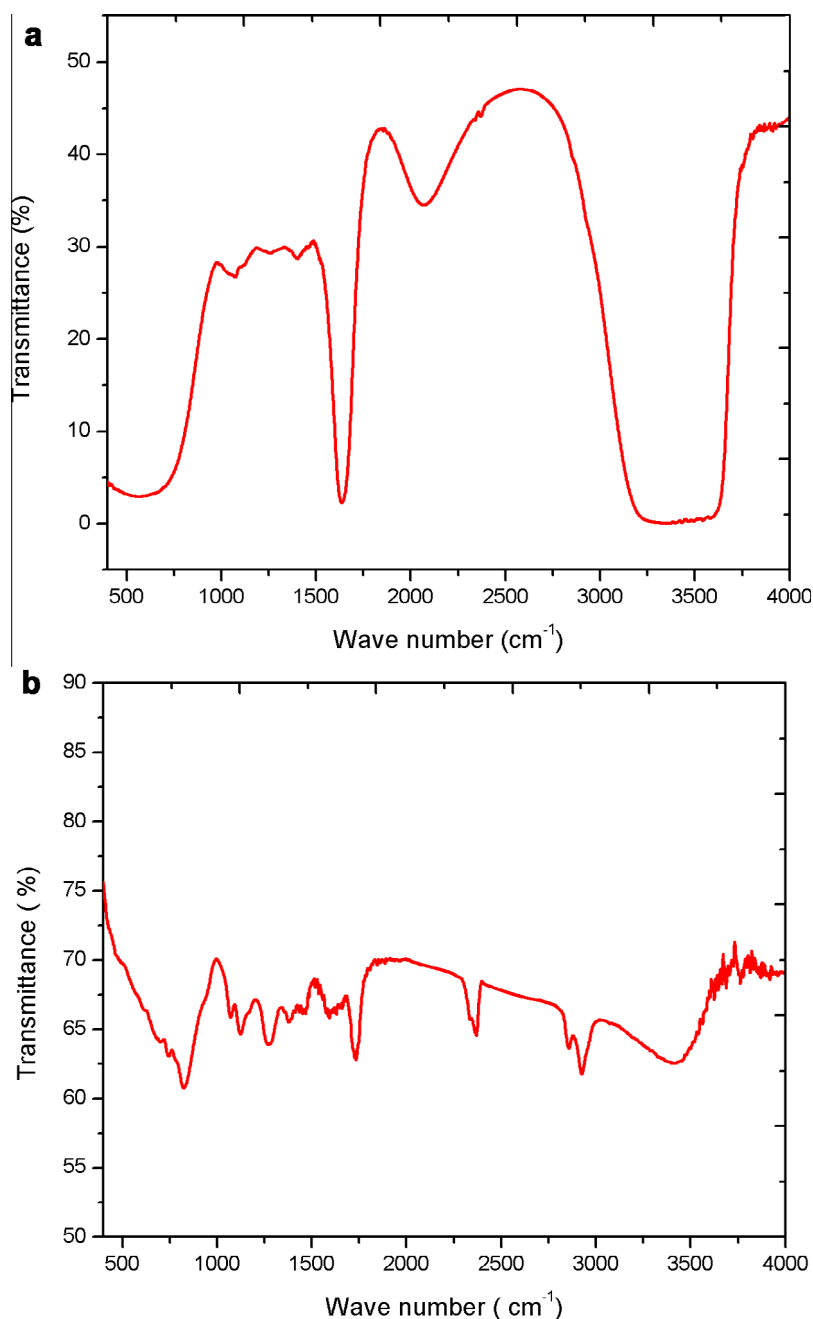


Figure 9 FT-IR spectra of (a) *Lannea coromandelica* leaf extract (b) adsorbed layer formed on the mild steel after immersion in 1 M H_2SO_4 containing LCLE.

$$\Delta G_{\text{ads}} = -RT \ln(55.5 K) \quad (9)$$

Here R is the gas constant, T is the absolute temperature and 55.5 is the concentration of water in the solution. The values of K were found to decrease with increasing temperature showing that the interactions between the adsorbed molecules and the metal surface are weakened and the inhibitor molecules become easily removable. Such data explain the decrease in the protection efficiency with increasing temperature. In the present work, the negative values of ΔG_{ads} (Table 4) clearly indicated the spontaneous adsorption of LCLE on mild steel surface and strong interactions between inhibitor molecules and the metal surface (Behpour et al., 2011; Boukalah et al.,

2006). Generally, the values of ΔG_{ads} up to -20 KJ/mol signify physisorption, which is consistent with electrostatic interaction between charged molecules and a charged metal. The values around -40 KJ/mol or higher involve charge sharing or transfer from the inhibitor molecules to the metal surface to form a co-ordinate type of bond (Behpour et al., 2011; Boukalah et al., 2006; Li et al., 2010; Gulsen Avci, 2008). In this study, the calculated values of ΔG_{ads} were less than -20 KJ/mol, indicating that the adsorption mechanism of LCLE on mild steel in 1 M sulfuric acid solution at the studied temperatures was physisorption (Gulsen Avci, 2008; Gunavathy and Murugavel, 2012; Eduok et al., 2012).

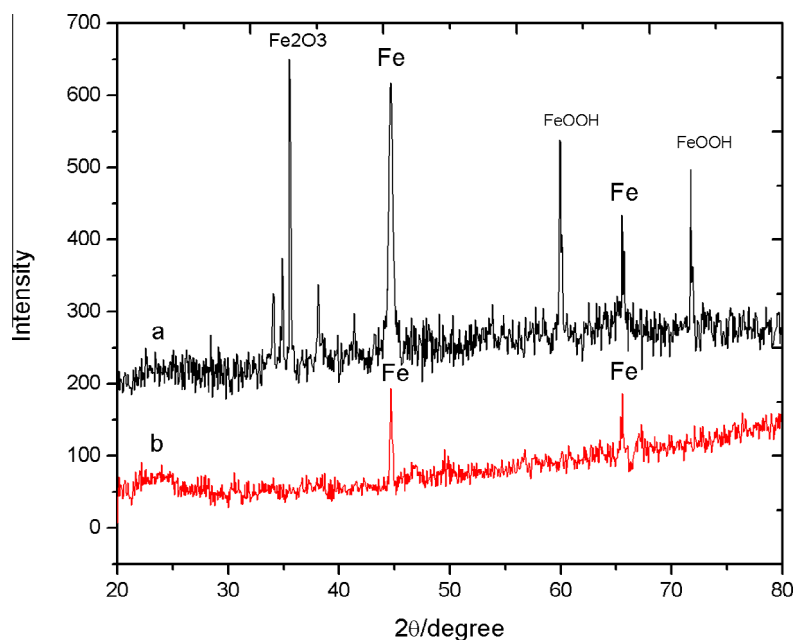


Figure 10 XRD spectrum of mild steel corrosion in the (a) absence (b) presence of LCLE.

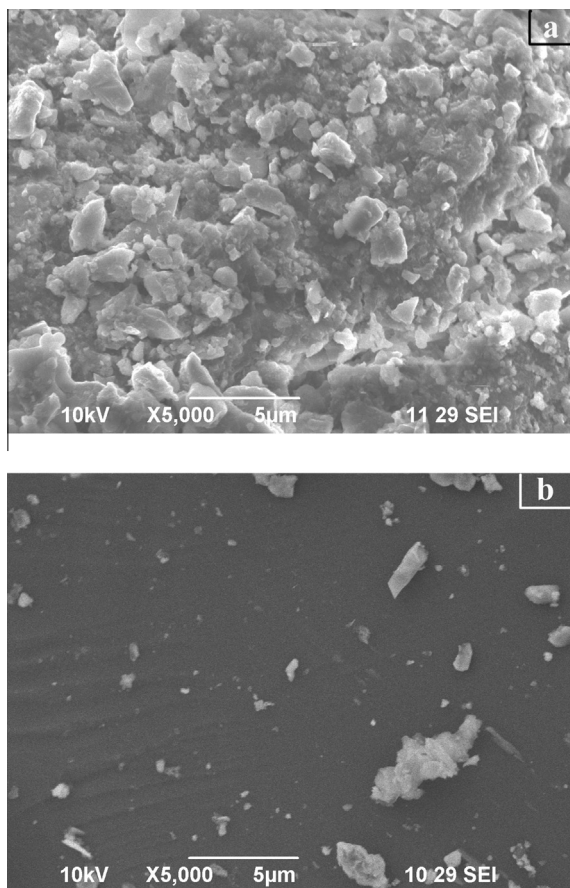


Figure 11 SEM images of mild steel in 1 M H_2SO_4 (a) without (b) with 250 mg/l of LCLE.

The heat of adsorption and entropy of adsorption are important parameters for understanding adsorption of organic inhibitors at metal/solution interface. The heat of adsorption (ΔH_{ads}) is calculated using the van't Hoff equation:

$$\ln K = -\Delta H_{ads}/RT + \text{constant} \quad (10)$$

Fig. 8 shows the straight lines of plot of $\ln K$ vs $1/T$ and slope of this straight line is equal to $-\Delta H_{ads}/R$. The heat of adsorption could be approximately regarded as the standard heat of adsorption (ΔH_{ads}) under experimental conditions. Now standard entropy of adsorption (ΔS_{ads}) is obtained by the thermodynamic basic equation:

$$\Delta S_{ads} = \frac{\Delta G_{ads} - \Delta H_{ads}}{T} \quad (11)$$

All the calculated thermodynamic parameters are listed in Table 4. It has been found that values of ΔH_{ads} are negative, suggesting that the adsorption of inhibitor is an exothermic process, which means lower inhibition efficiency at high temperature. This indicated the gradual desorption of inhibitors from the surface of mild steel (Li et al., 2012). All values of ΔS_{ads}° are negative, This behavior might be explained as follows: before the adsorption of inhibitor molecules onto the mild steel surface, inhibitor molecules might freely move in the bulk solution (inhibitor molecules were chaotic), but with the process of adsorption, inhibitor molecules were orderly adsorbed onto the steel surface, as a result a decrease in entropy is observed (Li et al., 2010, 2012).

3.5. FT-IR studies

FT-IR spectrum of LCLE is shown in Fig. 9a. Original absorption band at 3431 cm^{-1} (associated hydroxyl) was overlapped by the strong stretching mode of N-H. The 1635 cm^{-1} band was due to stretching mode of C=O. The peaks at 2073 cm^{-1} could be assigned to stretching mode of $-C=N$.

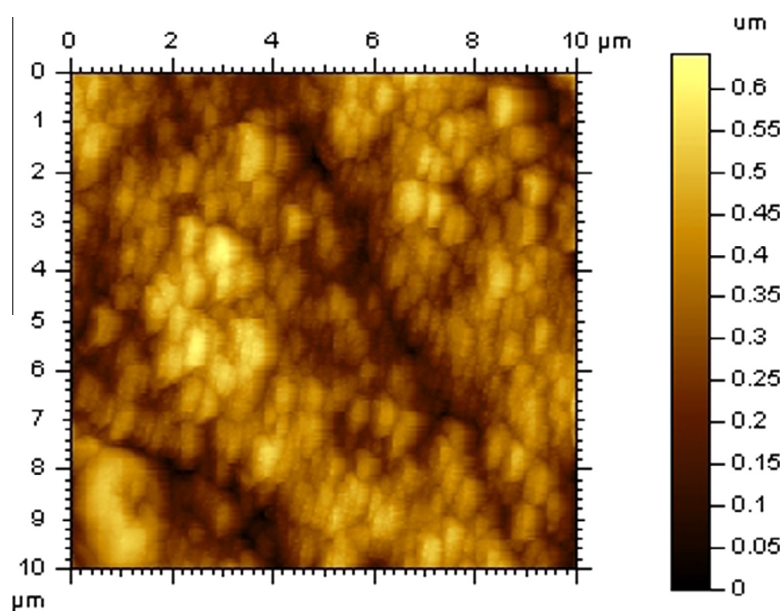


Figure 12 AFM topographical images of mild steel in 1 M H₂SO₄.

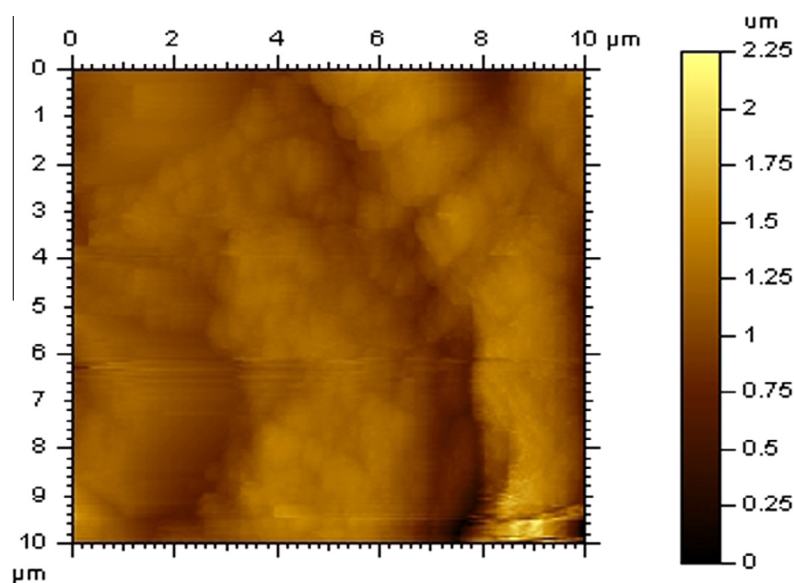


Figure 13 AFM topographical images of mild steel in 1 M H₂SO₄ with 250 mg/l of LCLE.

The peaks at 1465 cm^{-1} could be attributed to the stretching mode of aromatic substituted N=N. The peaks for C-C stretching and bending modes were noticed at 1381 and 1124 cm^{-1} respectively. The band at 1072 cm^{-1} might be due to the asymmetric stretching mode of C-O-C. These observations confirmed that the leaf extract contains a mixture of natural products. The FTIR spectrum of adsorbed protective layer formed on mild steel surface after immersion in 1 M H₂SO₄ containing 250 mg/l LCLE is shown in Fig. 9b. On comparing Fig 9a and b, it could be seen that certain additional peaks had appeared and some shifted to a higher frequency region, provided that some interaction/adsorption had taken place over the metal surface. The N-H stretching shifted from 3431 to 3423 cm^{-1} indicated the coordination of

inhibitor with Fe²⁺ through N atom of the N-H group. The shifting of C=O stretching from 1635 to 1734 cm^{-1} might confirm that there is a strong interaction between LCLE and the mild steel surface. All these results confirmed the adsorption of inhibitor on the surface of the mild steel (Ebenso et al., 2008b).

3.6. Analysis of the X-ray diffraction patterns

X-ray diffraction patterns were used to determine film formation of mild steel in various test solutions. The XRD pattern film formed on the surface of the mild steel immersed in sulfuric acid solution is shown in Fig. 10a. Peaks at $2\theta = 35.5^\circ$, 59.9° , 71.7° suggested the presence of iron oxide and a very

small amount of brown film due to Fe_2O_3 was observed visually. Fig 10b shows the X-ray diffraction patterns of mild steel immersed in the test solution containing 250 mg/l of LCLE. No brown film was observed visually. The peaks due to iron appeared at $2\theta = 44.6^\circ$ and 65.5° , which indicated the absence of oxides of iron (Fe_2O_3 , Fe_3O_4 and FeOOH). This result was in good agreement with the observations made by Abboudi et al. (2012a,b).

3.7. Scanning electron microscopic studies

Fig 11a and b shows the SEM images of mild steel surface after immersion in 1 M H_2SO_4 in the presence and absence of LCLE for 6 h. After 6 h, the specimens were taken out and dried. SEM images showed that the surface of the inhibited sample of mild steel specimens were better than the uninhibited sample. This examination indicated that the corrosion rate was reduced in the presence of inhibitors. This might be due to the adsorption of inhibitor molecules on the metal surface as a protective layer (Prabhu et al., 2009).

3.8. Atomic force microscope (AFM) surface examination

Atomic force microscope is a powerful technique to investigate the surface morphology studies which have been used to study the influence of inhibitors on the metal/solution interface (Solmaz, 2010; Wang et al., 2011). The topography AFM images of mild steel surface in 1.0 M H_2SO_4 in the absence and presence of 250 mg/l LCLE is given in Figs. 12 and 13. As is shown in Fig. 12, the surface of mild steel electrode exposed to 1 M H_2SO_4 solution had a considerable porous structure with large and deep pores. On the other hand, in the presence of an LCLE inhibitor, Fig 13 shows that the mild steel surface appears more flat, homogeneous and uniform, which indicated that LCLE shows an appreciable resistance to corrosion. Therefore, it could be concluded that the molecules of the leaf extract were adsorbed on the mild steel surface and protected the metal against corrosion.

3.9. Phytochemical screening of leaf extract

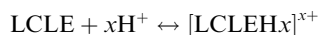
Phytochemical screening of the leaf extract showed the presence of flavonoids, glucosides, carbohydrates, phenols and tannins while alkaloids, aminoacids, steriods, triterpenoids, saponins were absent in the tested extracts (Table 5).

Table 5 Qualitative analysis of phytochemical compounds of *Lannea coromandelica*.

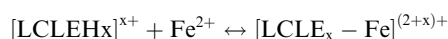
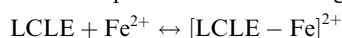
S.No	Phytochemical components	Aqueous extract
1.	Alkaloids	–
2.	Flavonoids	+
3.	Glucosides	+
4.	Carbohydrates	+
5.	Phenols	+
6.	Aminoacids	–
7.	Steriods	–
8.	Triterpenoids	–
9.	Saponins	–
10.	Tannins	+

3.10. Mechanism of inhibition

From the experimental and theoretical results obtained, the inhibition effect of LCLE in H_2SO_4 solution can be explained as follows:



In aqueous acidic solutions, the LCLE exists either as neutral molecules or in the form of cations (protonated LCLE). Generally, two modes of adsorption could be considered. The neutral LCLE may be adsorbed on the metal surface via the chemisorption mechanism involving the displacement of water molecules from the metal surface and the sharing of electrons between oxygen atom and iron. The LCLE molecules can be adsorbed also on the metal surface on the basis of donor–acceptor interactions between π -electrons of the heterocycle and vacant d-orbitals of iron. On the other hand, the protonated LCLE may be adsorbed through electrostatic interactions between the positive molecules and already adsorbed sulfate ions. Thus, the metal complexes of Fe^{2+} and LCLE or protonated LCLE might be formed as follows:



These complexes might be adsorbed on mild steel surface by the Vander Waals force to form a protective film to keep the mild steel surface from corrosion. Similar mechanism has been documented (Li et al., 2009).

4. Conclusion

The results presented in this paper showed that the extracts from LCL inhibited the corrosion of mild steel in 1 M H_2SO_4 . The inhibition efficiency of mild steel in 1 M H_2SO_4 increased with increasing the concentration of LCLE but decreased with increasing temperature. Potentiodynamic polarization measurements revealed that LCLE acted as a mixed type inhibitor but effect on the anodic reactions is more predominant. EIS measurement revealed that charge transfer increased with increase in concentration of LCLE, indicating that the inhibition increased with increase in concentrations. The adsorption of the inhibitor obeyed the Langmuir adsorption isotherm at all investigated temperatures. The adsorption was spontaneous and the inhibition of corrosion by LCLE was due to the formation of physical adsorption on the mild steel surface. Protective film formation against acid attack was confirmed by FTIR, XRD, SEM and AFM techniques. The results obtained from weight loss, polarization and impedance measurements are in good agreement.

References

- Abboudi, Y., Hammouti, B., Abourrichel, A., Ihssanel, B., Bennamar, A., Charroufi, M., Al-Deyab, S.S., 2012a. *Int. J. Electrochem. Sci.* 7, 2543–2551.
- Abboud, Y., Hammouti, B., Abourriche, A., Bennamara, A., Han-nache, H., 2012b. *Res. Chem. Intermed.* 38, 1591–1607.
- Amin, M.A., El-Sherbini, S.S.A., Bayoumy, R.S., 2007. *Electrochim. Acta* 52, 3588–3600.
- Atul Kumar, 2008. *E-J. Chem.* 5, 275–280.
- Kumar Reddy, Avinash, Jyothi, M.Joy, Ashok Kumar, C.K., 2011. *J. Pharm. Res.* 4, 577–579.

- Behpour, M., Ghoreishi, S.M., Khayatkashani, M., Soltani, N., 2011. *Corros. Sci.* 53, 2489–2501.
- Bentiss, F., Bouanis, M., Mernari, B., Traisnari, M., Vezin, H., Lagrenee, M., 2007. *Appl. Surf. Sci.* 253, 3696–3704.
- Brindha, P., Sasikala, K., Purushoth, K., 1977. *Ethnobot.* 3, 84–96.
- Boukalah, M., Hammouti, B., Lagrenee, M., Bentiss, F., 2006. *Corros. Sci.* 48, 2831–2837.
- Bouklah, M., Benchat, N., Hammouti, B., Aouniti, A., Kertit, S., 2006. *Mater. Lett.* 60, 1901–1905.
- Bouyanzer, A., Hammouti, B., Majidi, L., 2006. *Mater. Lett.* 60, 2840–2843.
- De Souza, F.S., Spinelli, A., 2009. *Corros. Sci.* 52, 642–649.
- Ebenso, E.E., Eddy, N.O., Odiongenyi, A.O., 2009. *Electrochim. Acta* 54, 13–22.
- Ebenso, E.E., Hailemichael, Umoren, S.A., Obot, I.B., 2008a. *Int. J. Electrochem. Sci.* 3, 1325–1339.
- Ebenso, E.E., Eddy, N.O., Odiongenyi, A.O., 2008b. *Afr. J. Pure Appl. Chem.* 2, 107–115.
- Eddy, N.O., Ebenso, E.E., 2008. *African J. Pure Appl. Chem.* 2, 46–54.
- Eduok, U.M., Umoren, S.A., Udoh, A.P., 2012. *Arabian J. Chem.* 5, 325–337.
- El-Etre, A.Y., 2007. *J. Colloid Interface Sci.* 314, 578–583.
- Fallavena, T., Antonow, M., Goncalves, R.S., 2006. *Appl. Surf. Sci.* 253, 566–571.
- Gomma, M.K., Wahdan, M.H., 1995. *Mater. Chem. Phys.* 39, 209–213.
- Goncalves, R.S., Mello, L.D., 2001. *Corros. Sci.* 43, 457–470.
- Guan, N.M., Xueming, L., Fei, L., 2004. *Mater. Chem. Phys.* 86, 59–68.
- Avcı, Gulsen., 2008. *Colloids Surf., A* 317, 730–736.
- Harbone, J.B., 1988. 3rd edition. Chapman and Hall, London, 1–138.
- Gunavathy, N., Murugavel, S.C., 2012. *E-J. Chem.* 9, 487–495.
- Ibrahim, T., Habbab, M., 2011. *Int. J. Electrochem. Sci.* 6, 5357–5371.
- Ita, B.I., Offiong, O.E., 1999. *Mater. Chem. Phys.* 59, 179–184.
- Lebrini, M., Robert, F., Lecante, A., Ross, C., 2011. *Corros. Sci.* 53, 687–695.
- Lecante, A., Robert, F., Blandinieres, P.A., Roos, C., 2011. *Curr. Appl. Phys.* 11, 714–724.
- Li, X.H., Deng, S.D., Fu, H., 2010. *Prog. Org. Coat.* 67, 420–426.
- Li, X.H., Deng, S.D., Fu, H., 2012. *Corros. Sci.* 62, 163–175.
- Li, X.H., Deng, S.D., Fu, H., Li, T., 2009. *Electrochim. Acta* 54, 4089–4098.
- Moretti, G., Guidi, F., Grion, G., 2004. *Corros. Sci.* 46, 387–403.
- Musa, A.Y., Mohamed, A.B., Takriff, M.S., Jalgham, R.T.T., 2012. *Res. Chem. Intermed.* 38, 453–461.
- Obot, I.B., Ebenso, E.E., Zuhair, M.Gasem, 2012. *Int. J. Electrochem. Sci.* 7, 1997–2008.
- Okafor, P.C., Ikpi, M.I., Uwah, I.E., Ebenso, E.E., Ekpe, U.J., Umoren, S.A., 2008. *Corros. Sci.* 50, 2310–2317.
- Oguzie, E.E., 2008. *Corros. Sci.* 50, 2993–2998.
- Oguzie, E.E., Onuoha, G.N., Onuchukwu, A.I., 2005. *Mater. Chem. Phys.* 89, 305–311.
- Popova, A., Christov, M., Raicheva, S., Sokolava, E., 2004. *Corros. Sci.* 46, 1333–1350.
- Prabhu, R.A., Venkatesha, T.V., Shanbhag, A.V., 2009. *J. Iranian Chem. Soc.* 6, 353–363.
- Ravi chandran, R., Rajendran, N., 2005. *Appl. Surf. Sci.* 241, 449–458.
- Sanja Martinez, Ivica Stern, 2002. *Appl. Surf. Sci.* 199, 83–89.
- Satapathy, A.K., Gunasekaran, G., Sahoo, S.C., Kumar, A., Rodrigues, P.V., 2009. *Corros. Sci.* 51, 2848–2856.
- Shahid, M., 2011. *Adv. Nat. Sci: Nanosci. Nanotechnol.* 2, 043001.
- Singh, A.K., Quraishi, M.A., 2010. *Mater. Chem. Phys.* 123, 666–677.
- Sobhi, M., Abdallah, M., Khairou, K.S., 2012. *Monatsh. Chem.* 143, 1379. <http://dx.doi.org/10.1007/s00706-011-0710-4>.
- Solmaz, R., 2010. *Corros. Sci.* 52, 3321–3330.
- Soltani, N., Behpour, M., Ghoreishi, H., Naeimi, S.M., 2010. *Corros. Sci.* 52, 1351–1361.
- Taleb, I., Mehad, H., 2011. *Int. J. Electrochem. Sci.* 6, 5357–5371.
- Vadivel et al, 2012. *Int. J. Pharmacol. Res.* 2, 64–68.
- Vinod kumar, K.P., Narayanan pillai, M.S., Rexin Thusnavis, G., 2010. *P Electrochim. Acta* 28, 373–383.
- Wang, B., Du, M., Zhang, J., Gao, C.J., 2011. *Corros. Sci.* 53, 353–361.
- Zhang, Q.B., Hua, Y.X., 2009. *Electrochim. Acta.* 54, 1881–1887.
- Zhang, D.Q., Cai, Q.R., Gao, L.X., Lee, K.Y., 2008. *Corros. Sci.* 50, 3615–3621.